Geology

High SO_2 flux, sulfur accumulation, and gas fractionation at an erupting submarine volcano

David A. Butterfield, Ko-ichi Nakamura, Bokuichiro Takano, Marvin D. Lilley, John E. Lupton, Joseph A. Resing and Kevin K. Roe

Geology 2011;39;803-806
doi: 10.1130/G31901.1

Notes

High SO_2 flux, sulfur accumulation, and gas fractionation at an erupting submarine volcano

David A. Butterfield[1], Ko-ichi Nakamura[2], Bokuichiro Takano[3], Marvin D. Lilley[4], John E. Lupton[5], Joseph A. Resing[1], and Kevin K. Roe[1]

[1]University of Washington, Joint Institute for the Study of the Atmosphere and Ocean (JISAO), Box 354925, Seattle, Washington 98195, USA

[2]National Institute of Advanced Industrial Science and Technology, Tsukuba, Ibaraki 3058567, Japan

[3]University of Tokyo, Graduate School of Arts and Sciences, Tokyo, Japan

[4] University of Washington, School of Oceanography, Box 357940, Seattle, Washington 98195, USA

[5]National Oceanic and Atmospheric Administration, Pacific Marine Environmental Laboratory (NOAA/PMEL), 2115 SE OSU Drive, Newport, Oregon 97365, USA

ABSTRACT

Strombolian-style volcanic activity has persisted for six years at the NW Rota-1 submarine volcano in the southern Mariana Arc, allowing direct observation and sampling of gas-rich fluids produced by actively degassing lavas, and permitting study of the magma-hydrothermal transition zone. Fluids sampled centimeters above erupting lava and percolating through volcaniclastic sediments around an active vent have dissolved sulfite >100 mmol/kg, total dissolved sulfide <30 µmol/kg, pH as low as 1.05, and dissolved Al and Fe >1 mmol/kg. If NW Rota is representative of submarine arc eruptions, then volcanic vent fluids from seawater-lava interaction on submarine arcs have a significant impact on the global hydrothermal flux of sulfur and Al to the oceans, but a minimal impact on Mg removal. Gas ratios (SO_2, CO_2, H_2, and He) are variable on small spatial and temporal scales, indicative of solubility fractionation and gas scrubbing. Elemental sulfur (S_e) is abundant in solid and molten form, produced primarily by disproportionation of magmatic SO_2 injected into seawater. S_e accumulates within the porous rock surrounding the lava conduit connecting the magma source to the seafloor. Accumulated S_e can be heated, melted, and pushed upward by rising magma to produce molten S_e flows and lavas saturated with S_e. Molten S_e near the top of the lava conduit may be ejected up into the water column by escaping gases or boiling water. This mechanism of S_e accumulation and refluxing may underlie the relatively widespread occurrence of S_e deposits of many sizes found on submarine arc volcanoes.

INTRODUCTION

Because mid-ocean ridge (MOR) volcanic eruptions have proved to be unpredictable and short in duration (Haymon et al., 1993; Embley et al., 1995), deep-sea eruptions and the magma degassing that accompany them have remained hidden beneath the ocean surface until very recently (Embley et al., 2006; Chadwick et al., 2008). The dramatic but generally inaccessible physicochemical gradients within the transition zone between magma and water-saturated rock hold critical information for understanding volcanic eruptions, magma degassing, and their contributions to hydrothermal systems. Magma degassing within the oceanic crust is common, based on excess CO_2 in vent fluids (Butterfield et al., 1990; Lilley et al., 2003; Lupton et al., 2006, 2008), but there has been no previous opportunity to observe degassing and sample magmatic gases and fluids directly on the seafloor. Here we show that a long-lived eruption at submarine volcano NW Rota-1 on the Mariana Arc (Embley et al., 2006) has exposed the magma-hydrothermal boundary under conditions that allow sampling of gases and hydrothermal solutions <1 m above degassing magma.

Results from our study indicate that there is rapid fractionation of sulfur, carbon, and trace gases at the site of degassing, and that elemental sulfur (S_e) accumulates and refluxes over the magma conduit. The balance between H_2S and SO_2, the two dominant magmatic sulfur gases, yields information about the oxidation state of erupting lavas. The high ratio of excess sulfur to heat from volatile-rich submarine volcanic arc eruptions may have a significant impact on the global oceanic sulfur balance. Due to their extreme acidity, fluids produced by submarine volcanic arc eruptions have an inordinately large impact on the global hydrothermal Al flux. High H_2 and SO_2 and strong acidity also create substantially different habitat conditions for biological communities living on active arc volcanoes relative to mid-ocean ridges.

GEOLOGIC SETTING AND SAMPLING

NW Rota-1 is a submarine volcano located at 14°36′N, 144°45′E on the Mariana Arc near the islands of Rota and Guam. Since its discovery in 2003, NW Rota has been in a state of near-continuous, Strombolian-style eruption (Embley et al., 2006; Chadwick et al., 2008; Deardorff et al., 2011). In 2004, 2006, and 2009 we used a specialized hydrothermal sampling device with in-line temperature measurement attached to the remotely operated vehicles *ROPOS* and *Jason-2* to collect fluids from the volcanic vent at NW Rota (methods are presented in the GSA Data Repository[1]). In 2004, the volcano was in a state of slow and intermittent eruption characterized by bursts of gas, molten sulfur, and basaltic andesite (R. Stern, 2008, personal commun.) fragments from a deep and narrow eruptive vent given the name Brimstone. Buoyant 30 °C fluids were captured at 550 m depth, ~15–20 m above the bottom of the pit. In 2006, a second expedition sampled gases (Lupton et al., 2008) and hot fluids around and directly over actively erupting and degassing lava at 550 m depth. Volcanic fluid samples were taken within 50 cm or less of the surface of erupting, degassing lava and are the most concentrated fluids that could be collected from the volcanic vent. Brimstone was sampled for a third time in April 2009, when the vent activity was near the summit of a newly built cone at 520 m depth. The ambient pressure at the summit of NW Rota is significantly less than the critical pressure for water, so the magmatic fluids are vapor and not brine.

RESULTS AND DISCUSSION

We measured concentrations of dissolved sulfite [SO_2(aq)] ranging from 10 µM to 163 mM in vent fluids collected from Brimstone and nearby vents (Fig. 1; Table DR1 in the Data Repository). The highest concentrations were found immediately over actively erupting lavas and in acidic (pH 1.05), gas- and particle-rich vents on the edges of active eruptions. Total H_2S

[1]GSA Data Repository item 2011237, sampling and analytical methods description; Table DR1 (2009 sulfur chemistry); Table DR2 (list of fluid samples); Table DR3 (chemical composition of fluid samples); Table DR4 (2004/2006 aqueous sulfur species composition); Figures DR1–DR7; and Video DR1 (video of a small crater at Brimstone), is available online at www.geosociety.org/pubs/ft2011.htm, or on request from editing@geosociety.org or Documents Secretary, GSA, P.O. Box 9140, Boulder, CO 80301, USA.

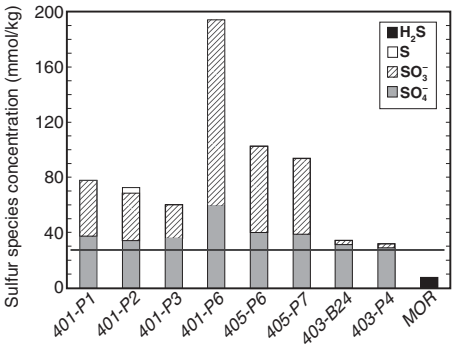

Figure 1. Major sulfur species composition (Table DR1; see footnote 1) of volcanic vent fluid samples collected in 2009 from Brimstone at NW Rota-1 submarine volcano. S is particulate elemental sulfur. Sample numbers listed below bars. Average high-temperature mid-ocean ridge (MOR) vent composition at far right for comparison. Measured H_2S concentrations were below detection limits or too small to be visible on this plot. Horizontal line indicates seawater sulfate; sulfate above this line is excess. All samples have significant excess sulfur, primarily as sulfite. Average oxidation number of excess dissolved sulfur is 4.5.

concentration is very low in the Brimstone samples (Table DR1). The fluids collected for this study (Table DR2) have millimolar levels of Fe, Al, and Si, with Fe/Mn ratios as high as 55, similar to the ratio in fresh rock (Table DR3; Figs. DR1–DR3). Mg in the fluids remains within a few percent of the seawater concentration (Table DR3).

These volcanic eruptive fluids have a high water/rock ratio and are unlike zero-Mg, high-temperature MOR fluids derived from seawater reacting and approaching equilibrium with hot rock at a water/rock ratio of ~1 (Seyfried, 1987). The most striking differences are that Mg is not removed, Al is highly enriched, and the speciation of sulfur is unlike anything found on the MOR. Recent sulfur species measurements on a second erupting arc volcano (West Mata, northeast Lau Basin) are similar to the results for NW Rota (Butterfield's unpublished data). All of these features indicate that the volcanic vent fluids are derived from rapid, shallow reaction of hot, condensed magmatic gases with seawater and volcanic rock.

Magmatic-Hydrothermal Sulfur Chemistry

SO_2(g) is a major component of high-temperature magmatic gas and can be the dominant form of sulfur gas (Moretti and Papale, 2004). SO_2 has been inferred to be the source of excess sulfate and acidity in vent fluids from the Manus Basin (Gamo et al., 1997) and similarly as the main source of acidity in the plume over NW Rota (Resing et al., 2007), but direct measurements of SO_2(aq) in vent fluids have not been previously reported. SO_2 gas is highly soluble in water, but SO_2(aq) is thermodynamically unstable under hydrothermal conditions (temperature <350 °C), where H_2S is the dominant form of sulfur (Seyfried, 1987; Giggenbach, 1987; Symonds et al., 2001), and models often assume that SO_2(aq) is insignificant (Symonds et al., 1992, 2001). Aqueous SO_2 can undergo the following reactions:

$$SO_2(aq) + H_2O = HSO_3^- + H^+, \quad (1)$$

$$3SO_2(aq) + 2H_2O = S_e + 2H_2SO_4, \quad (2)$$

$$4SO_2(aq) + 4H_2O = H_2S + 3H_2SO_4. \quad (3)$$

SO_2 rapidly hydrates to form sulfurous acid, which in turn dissociates to yield dissolved bisulfite (reaction 1) and sulfite ions. SO_2 (+IV oxidation state) may also disproportionate in water to yield H_2SO_4 (+VI) and either S_e (0 oxidation state, reaction 2) or H_2S (–II, Reaction 3).

SO_2 (detected as dissolved HSO_3^-), H_2SO_4, and S_e are the dominant forms of sulfur emitted at the volcanic vents (Fig. 1), indicating that Reactions 1 and 2 prevail over Reaction 3 when condensed magmatic gases rapidly mix with oxygenated ambient seawater. The persistence of SO_2(aq) in water samples after many hours at ambient temperature indicates slow post-sampling reaction rates. H_2S and SO_2 may coexist in the gas phase (Giggenbach, 1987; Aiuppa et al., 2005) and in volcanic lakes (Takano et al., 2004), with SO_2 dominating under magmatic temperatures (Giggenbach, 1987). Low levels of nongaseous thiosulfate ion ($S_2O_3^-$) in Brimstone fluid samples (Table DR4) suggest that the condensed gas has undergone minimal aqueous phase reaction. Therefore, the near-absence of H_2S in sampled fluids is best explained by a lack of H_2S in the primary magmatic gas. SO_2 quenching experiments (Kusakabe et al., 2000) support the interpretation that SO_2-rich condensed gases injected directly into seawater will favor formation of S_e and H_2SO_4 (reaction 2). Lower total dissolved SO_2, slightly higher pH, and rock-buffered redox conditions below the seafloor would favor H_2S as a product (reaction 3).

The relative proportions of magmatic SO_2 and H_2S are predicted to depend on the pressure, temperature, and redox condition of the magma (Giggenbach, 1987; Jugo et al., 2010; Moretti and Papale, 2004; Symonds et al., 2001). Arc lavas are more oxidizing than mid-oceanic ridge basalt (MORB), with higher Fe(III)/total Fe ratios and correlated high water content (Kelley and Cottrell, 2009). Consequently, arc magmas can dissolve five to seven times more total sulfur than MORB at sulfide saturation (Jugo et al., 2010), potentially leading to enhanced extraction of S from the mantle and contributing to high sulfur flux from arc volcanoes. If the high SO_2/H_2S ratio (>10^4) found in Brimstone volcanic fluids is due to heterogeneous magma-gas equilibrium, then this places the redox state of NW Rota magma between the magnetite-hematite and Ni-NiO (NNO) buffers (Symonds et al., 1992; Moretti and Papale, 2004). The average log[CO_2]/[CO] at Brimstone in 2006 was 2.8, higher than the value of 2.2 predicted by the NNO buffer at 50 atm, 1050 °C (Symonds et al., 1992), and also consistent with a more oxidized magma.

Gas Fractionation and Sulfur Accumulation

When the major volatile compounds making up >98% of the magmatic gas phase (H_2O, CO_2, SO_2 or H_2S, N_2, H_2, and minor S_2) are injected into cold seawater, they are subject to extreme fractionation based on their solubilities in water, which span nearly five orders of magnitude (order of solubility: $SO_2 > H_2S > CO_2 > CH_4 \geq H_2$) (Drummond, 1981). Water vapor and acid-producing SO_2 rapidly enter the aqueous phase while H_2, CO_2, and the less soluble trace gases initially remain as a separate gas (bubble) phase (Fig. 2), which is abundant at NW Rota (Chadwick et al., 2008; Lupton et al., 2008), seeping out of accumulated volcaniclastic material (basaltic andesite plus sulfur) and bursting out of exploding lava. Gas bubbles also escape in pulses around the edges of the volcanic vent, indicating that the source of the gas is the lava conduit connecting the magma chamber to the seafloor (Fig. 2). The gas solubility differences produce particle-rich fluids at Brimstone with gas content averaging 86.5% CO_2, 9.1% S gas (dominated by SO_2), and 2.2% H_2, while free gas bubbles sampled near the volcanic vent are ~90% CO_2 and 10% H_2 (Lupton et al., 2008) with no appreciable sulfur gas content.

The buoyant magmatic gas bubble phase is further fractionated as it rises through the water and migrates up through the porous water-saturated rock around the lava conduit, becoming depleted in the more soluble gases. After losing nearly all sulfur gas and some CO_2, the average free gas phase collected at Brimstone has CO_2/H_2 and CO_2/He ratios that are 5.9 and 6.8 times lower than in the average sulfur- and gas-rich aqueous samples from Brimstone. Because of this rapid fractionation based on solubility (Fig. 2), it is not simple to measure gas ratios (e.g., S/C or CO_2/He) of the primary magmatic gas.

Further fractionation occurs as insoluble S_e precipitates from acidic fluids (reaction 2) produced by injection of magmatic SO_2 into sea-water. Elemental sulfur is abundant at Brimstone vent, in fine particulate, massive solid, and molten forms (Figs. DR4–DR7). In one spectacular case, a small crater at Brimstone appeared to be full of molten S_e and boiling water (VideoDR1). Although the visual impres-

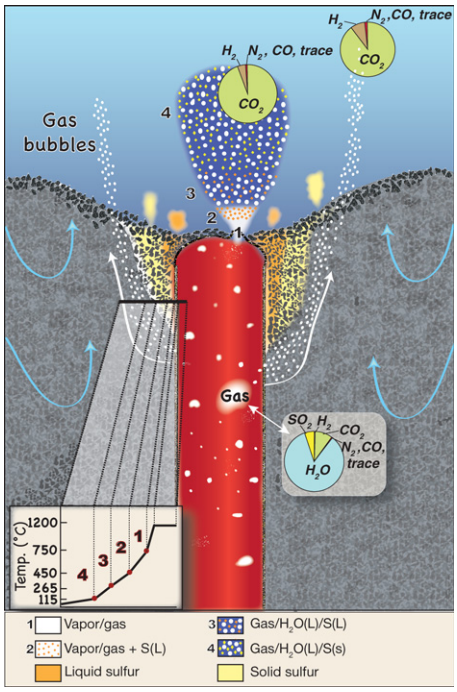

Figure 2. Schematic of chemical processes surrounding degassing lava conduit. Magma ascends slowly and gas pockets more rapidly in Strombolian-style eruption. Magmatic gases with primary composition (H_2O-CO_2-SO_2-H_2-S_2 trace gas; pie chart inset) escape vertically when gas pockets reach top of conduit and laterally when conduit walls are breached. H_2S is not significant portion of primary magmatic gas. Magma-to-seawater temperature gradient (numbered zones linked to transect) imposes structure common to sulfur-rich degassing systems. 1. Water-rich gas escapes magma near brittle-ductile transition temperature (~750 °C). 2. Magmatic S_2(g) condenses to form sulfur liquid in water vapor medium near 450 °C. 3. Water vapor condenses to liquid at two-phase boundary (~265° at NW Rota), producing hot solution of sulfurous acid; disproportionation reactions begin, and CO_2-rich gas phase separates; strong acid dissolves rock. 4. Sulfur liquid freezes to solid near 115 °C. After SO_2 dissolves in water, remaining sulfur-depleted gases (~90% CO_2/5% H_2 with minor methane and trace gases) ascend (white arrows) through porous rock surrounding conduit and exit seafloor as free gas bubbles. Solubility fractionation (scrubbing) makes free gas phase relatively depleted in more soluble gases. Liquid (orange) and solid (yellow) elemental sulfur (S_e) accumulates around and over top of conduit, and may be remelted or vaporized and driven out the top of conduit when magma ascends. Explosive bursts eject molten S_e into seawater, forming S_e spherules. Because of the insolubility and density of molten and solid S_e and the filtering capacity of porous volcanic deposits, only fine particulate S_e will escape with circulating water. Seawater (blue arrows) circulates freely through highly porous and permeable rock, maintaining high water/rock ratio and rapid cooling around volcanic vent.

sion is that fine particulate S_e is created immediately as magmatic gas escapes into seawater at the volcanic vents, explosive activity and interaction of ascending lava with accumulated S_e may produce this same S_e "smoke" as well as S_e droplets and intense yellow S_e plumes.

The physical separation of S, metals, and heat from insoluble gas bubbles at the volcanic vent creates a dual source to the overlying water column and complicates the efforts to infer seafloor source properties (especially gas ratios or gas/heat ratios) from hydrothermal plume properties. Sheets of gas bubbles noted by Chadwick et al. (2008) have been imaged by sonar rising hundreds of meters above the volcano summit (Hughes-Clark et al., 2009), potentially transporting magmatic gases into the surface ocean. However, continued fractionation and gas exchange during bubble rise (Leifer and Patro, 2002) make the contribution to surface ocean chemistry uncertain.

The rapid fractionation of sulfur, carbon, and trace gases with accumulation of S_e over the magma source may explain observations at other volatile-rich submarine volcanoes where excess carbon and sulfur accumulate. When the degassing magma body is farther below the volcano-water interface, injection of magmatic gas into the water-saturated, permeable rock above the magma chamber would quickly result in the fractionation of gases with the formation of a sulfur-rich zone over the magma source and CO_2 escaping into cooler water above. The fractionation of CO_2 from SO_2 by differential aqueous solubility likely underlies the formation of cooled liquid CO_2 observed at two sites in the western Pacific (Lupton et al., 2006; Sakai et al., 1990; Konno et al., 2006), while the recent discovery of molten S_e lakes and S_e-filled calderas (Embley et al., 2007) are likely explained by larger scale refluxing of S_e accumulated by the same mechanism.

Impact on Global Hydrothermal Fluxes

Acidic, volatile-rich fluids produced by erupting submarine arc volcanoes may change estimates of global hydrothermal fluxes. Concentration anomalies in fluids can be normalized to heat content using the in-line temperatures recorded during sampling. NW Rota fluids have an average of 275 (±113) nmol/J excess dissolved sulfur (Table DR1), much larger than the average net dissolved sulfur loss of 13 nmol/J for a broad range of MOR vent fluids. Submarine volcanic arcs produce 10% of the global hydrothermal heat flux (Baker et al., 2008), and to balance all of the sulfur lost during on-axis MOR circulation would require the arc eruptive heat flux to be 40% of the total arc heat flux. This is possible given that ratios of intrusive to extrusive magma production are estimated at 1:1–3:1 for several volcanic arc environments (White et al., 2006). Although results from a single submarine volcano must be considered preliminary, an estimate using 2.5%–5% of the global MOR axis hydrothermal heat flux (1.04×10^{19} J/yr; Stein and Stein, 1994) and our excess sulfur to heat ratio yields a range of $0.7–1.4 \times 10^{11}$ mol/yr SO_2 flux from submarine arc eruptions, comparable in magnitude to the global subaerial volcanic arc SO_2 flux of 3.15×10^{11} mol/yr (Fischer, 2008). Even if volcanic eruptions produced as little as 1% of the arc heat flux, they would still dominate the global hydrothermal flux of Al to the oceans because of the extremely high Al content (Al/heat >1000 times higher than MOR fluids; Table DR3), illustrating the importance of this previously unsampled class of volcanic fluids.

CONCLUSIONS

We have directly sampled the magma-hydrothermal transition zone during an active deep-sea eruption on the Mariana volcanic arc. SO_2 is the predominant form of magmatic sulfur gas and hydrothermal pathways at the volcanic vent are too short to produce H_2S. The highly soluble SO_2 dissolves in seawater to produce strongly acidic solutions and S_e, while less soluble gases escape as bubbles and are scrubbed as they rise through the water. Rapid reaction of the resulting hot, acidic solutions with volcanic rock produces volcanic vent fluids that affect the global hydrothermal fluxes of sulfur and Al.

ACKNOWLEDGMENTS

This research was supported by the National Oceanic and Atmospheric Administration (NOAA) Pacific Marine Environmental Laboratory (PMEL) Vents Program, the Joint Institute for the Study of the Atmosphere and Oceans, NOAA Ocean Exploration and Research, and the National Science Foundation (OCE-0751699). This is PMEL contribution 3498. Eric Olson, Ben Larson, Leigh Evans, and My Christensen analyzed samples. Karen Birchfield crafted Figure 2. Bob Stern provided rock composition data. Bob Embley and Bill Chadwick commented on the manuscript. Discussions with K. Cashman, N. Deardorff, E. Baker, and C. de Ronde were valuable. The expertise of the *ROPOS* and *Jason-2* groups are greatly appreciated.

REFERENCES CITED

Aiuppa, A., Inguaggiato, S., McGonigle, A.J.S., O'Dwyer, M., Oppenheimer, C., Padgett, M.J., Rouwet, D., and Valenza, M., 2005, H_2S fluxes from Mt. Etna, Stromboli, and Vulcano (Italy) and implications for the sulfur budget at volcanoes: Geochimica et Cosmochimica Acta, v. 69, p. 1861–1871, doi:10.1016/j.gca.2004.09.018.

Baker, E.T., Embley, R.W., Walker, S.L., Resing, J.A., Lupton, J.E., Nakamura, K.-I., de Ronde, C.E.J., and Massoth, G.J., 2008, Hydrothermal activity and volcano distribution along the Mariana Arc: Journal of Geophysical Research, v. 113, B08S09, doi:10.1029/2007JB005423.

Butterfield, D.A., Massoth, G.J., McDuff, R.E., Lupton, J.E., and Lilley, M.D., 1990, Geochemistry of hydrothermal fluids from Axial Seamount Hydrothermal Emissions Study Vent Field, Juan de Fuca Ridge: Subseafloor boiling and

subsequent fluid-rock interaction: Journal of Geophysical Research, v. 95, no. B8, p. 12,895–12,921, doi:10.1029/JB095iB08p12895.

Chadwick, W.W., Jr., Cashman, K.V., Embley, R.W., Matsumoto, H., Dziak, R.P., de Ronde, C.E.J., Lau, T.K., Deardorff, N.D., and Merle, S.G., 2008, Direct video and hydrophone observations of submarine explosive eruptions at NW Rota-1 Volcano, Mariana Arc: Journal of Geophysical Research, v. 113, B08S10, doi:10.1029/2007JB005215.

Deardorff, N.D., Cashman, K.V., and Chadwick, W.W., Jr., 2011, Observations of eruptive plumes and pyroclastic deposits from submarine explosive eruptions at NW Rota-1, Mariana Arc: Journal of Volcanology and Geothermal Research, doi:10.1016/j.jvolgeores.2011.01.003 (in press).

Drummond, S.E., 1981, Boiling and mixing of hydrothermal fluids: Chemical effects on mineral precipitation [Ph.D. thesis]: Pennsylvania State University, 381 p.

Embley, R.W., Chadwick, W.W., Jr., Jonasson, I.R., Butterfield, D.A., and Baker, E.T., 1995, Initial results of a rapid response to the 1993 CoAxial event: Relationships between hydrothermal and volcanic processes: Geophysical Research Letters, v. 22, p. 143–146, doi:10.1029/94GL02281.

Embley, R.W., and 16 others, 2006, Long-term eruptive activity at a submarine arc volcano: Nature, v. 441, no. 7092, p. 494–497, doi:10.1038/nature04762.

Embley, R.W., Baker, E.T., Butterfield, D.A., Chadwick, W.W., Jr., Lupton, J.E., Resing, J.A., de Ronde, C.E.J., Nakamura, K.-I., Tunnicliffe, V., Dower, J.F., and Merle, S.G., 2007, Exploring the submarine ring of fire: Mariana Arc–Western Pacific: Oceanography, v. 20, no. 4, p. 68–79.

Fischer, T.P., 2008, Fluxes of volatiles (H_2O, CO_2, N_2, Cl, F) from arc volcanoes: Geochemical Journal, v. 42, p. 21–38.

Gamo, T., Okamura, K., Charlou, J.L., Urabe, T., Auzende, J.M., Ishibashi, J.-I., Shitashima, K., and Chiba, H., 1997, Acidic and sulfate-rich hydrothermal fluids from the Manus back-arc basin, Papua New Guinea: Geology, v. 25, p. 139–142, doi:10.1130/0091-7613(1997)025<0139:AASRHF>2.3.CO;2.

Giggenbach, W.F., 1987, Redox processes governing the chemistry of fumarolic gas discharges from White Island, New Zealand: Applied Geochemistry, v. 2, p. 143–162.

Haymon, R.M., and 14 others, 1993, Volcanic eruption of the mid-ocean ridge along the East Pacific Rise crest at 9°45–52′N: Direct submersible observations of seafloor phenomena associated with an eruption event in April, 1991: Earth and Planetary Science Letters, v. 119, p. 85–101, doi:10.1016/0012-821X(93)90008-W.

Hughes Clark, J.E., Martinolich, R., and Broadus, M., 2009, Repetitive surface-mounted multibeam water column imaging of hydrothermal vent plumes over NW Rota 1: Eos (Transactions, American Geophysical Union), fall meeting, abs. V51D–1716.

Jugo, P.J., Wilke, M., and Botcharnikov, R.E., 2010, Sulfur K-edge XANES analysis of natural and synthetic basaltic glasses: Implications for S speciation and S content as function of oxygen fugacity: Geochimica et Cosmochimica Acta, v. 74, p. 5926–5938, doi:10.1016/j.gca.2010.07.022.

Kelley, K.A., and Cottrell, E., 2009, Water and the oxidation state of subduction zone magmas: Science, v. 325, p. 605–607, doi:10.1126/science.1174156.

Konno, U., Tsunogai, U., Nakagawa, F., Nakaseama, M., Ishibashi, J.I., Nunoura, T., and Nakamura, K.I., 2006, Liquid CO_2 venting on the seafloor: Yonaguni Knoll IV hydrothermal system, Okinawa Trough: Geophysical Research Letters, v. 33, L16607, doi:10.1029/2006GL026115.

Kusakabe, M., Komoda, Y., Takano, B., and Abiko, T., 2000, Sulfur isotopic effects in the disproportionation reaction of sulfur dioxide in hydrothermal fluids: Implications for the $\delta^{34}S$ variations of dissolved bisulfate and elemental sulfur from active crater lakes: Journal of Volcanology and Geothermal Research, v. 97, p. 287–307, doi:10.1016/S0377-0273(99)00161-4.

Leifer, I., and Patro, R.K., 2002, The bubble mechanism for methane transport from the shallow seabed to the surface: A review and sensitivity study: Continental Shelf Research, v. 22, p. 2409–2428, doi:10.1016/S0278-4343(02)00065-1.

Lilley, M.D., Butterfield, D.A., Lupton, J.E., and Olson, E.J., 2003, Magmatic events can produce rapid changes in hydrothermal vent chemistry: Nature, v. 422, no. 6934, p. 878–881, doi:10.1038/nature01569.

Lupton, J.E., and 15 others, 2006, Submarine venting of liquid carbon dioxide on a Mariana Arc volcano: Geochemistry Geophysics Geosystems, v. 7, Q08007, doi:10.1029/2005GC001152.

Lupton, J.E., Lilley, M.D., Butterfield, D.A., Evans, L.J., Embley, R.W., Massoth, G.J., Christenson, B., Nakamura, K.-I., and Schmidt, M., 2008, Venting of a separate CO_2-rich gas phase from submarine arc volcanoes: Examples from the Mariana and Tonga-Kermadec arcs: Journal of Geophysical Research, v. 113, B08S12, doi:10.1029/2007JB005467.

Moretti, R., and Papale, P., 2004, On the oxidation state and volatile behavior in multicomponent gas-melt equilibria: Chemical Geology, v. 213, p. 265–280, doi:10.1016/j.chemgeo.2004.08.048.

Resing, J.A., Lebon, G., Baker, E.T., Lupton, J.E., Embley, R.W., Massoth, G.J., Chadwick, W.W., Jr., and de Ronde, C.E.J., 2007, Venting of acid-sulfate fluids in a high-sulfidation setting at NW Rota-1 submarine volcano on the Mariana Arc: Economic Geology and the Bulletin of the Society of Economic Geologists, v. 102, p. 1047–1061, doi:10.2113/gsecongeo.102.6.1047.

Sakai, H.T., Gamo, T., Kim, E.S., Tsutsumi, M., Tanaka, T., Ishibashi, J., Wakita, H., Yamano, M., and Oomori, T., 1990, Venting of carbon dioxide-rich fluid and hydrate formation in mid-Okinawa Trough backarc basin: Science, v. 248, p. 1093–1096, doi:10.1126/science.248.4959.1093.

Seyfried, W.E., Jr., 1987, Experimental and theoretical constraints on hydrothermal alteration at mid-ocean ridges: Annual Review of Earth and Planetary Sciences, v. 15, p. 317–335, doi:10.1146/annurev.ea.15.050187.001533.

Stein, C.A., and Stein, S., 1994, Constraints on hydrothermal heat-flux through the oceanic lithosphere from global heat flow: Journal of Geophysical Research, v. 99, p. 3081–3095, doi:10.1029/93JB02222.

Symonds, R.B., Reed, M.H., and Rose, W.I., 1992, Origin, speciation, and fluxes of trace-element gases at Augustine volcano, Alaska: Insights into magma degassing and fumarolic processes: Geochimica et Cosmochimica Acta, v. 56, p. 633–657, doi:10.1016/0016-7037(92)90087-Y.

Symonds, R.B., Gerlach, T.M., and Reed, M.H., 2001, Magmatic gas scrubbing: Implications for volcano monitoring: Journal of Volcanology and Geothermal Research, v. 108, p. 303–341, doi:10.1016/S0377-0273(00)00292-4.

Takano, B., Suzuki, K., Sugimori, K., Ohba, T., Fazlullin, S.M., Bernard, A., Sumarti, S., Sukhyar, R., and Hirabayashi, M., 2004, Bathymetric and geochemical investigation of Kawah Ijen Crater Lake, East Java, Indonesia: Journal of Volcanology and Geothermal Research, v. 135, p. 299–329, doi:10.1016/j.jvolgeores.2004.03.008.

White, S.M., Crisp, J.A., and Spera, F.J., 2006, Long-term volumetric eruption rates and magma budgets: Geochemistry Geophysics Geosystems, v. 7, Q03010, doi:10.1029/2005GC001002.

Manuscript received 12 November 2010
Revised manuscript received 15 March 2011
Manuscript accepted 28 March 2011

Printed in USA

GSA DATA REPOSITORY 2011237

High SO_2 flux, sulfur accumulation, and gas fractionation at an erupting submarine volcano

David A. Butterfield, Ko-ichi Nakamura, Bokuichiro Takano, Marvin D. Lilley, John E. Lupton, Joseph A. Resing, Kevin K. Roe

Supplementary Methods

Hydrothermal fluids were sampled using the Hydrothermal Fluid and Particle Sampler (HFPS). HFPS pumps fluids through a titanium intake nozzle (Supplementary Figure 5) with an in-line temperature sensor, into a teflon and titanium manifold with 24 ports, then out through a 4-liter/minute pump to an exhaust port. An insulated one-meter extension to the titanium nozzle was used for highly energetic volcanic vent sampling. While the flush pump maintained fluid flow through the manifold, a dedicated sample pump pulled the fluid into selected sample containers, which were either PVC plastic cylinders with Teflon seals, titanium cylinders with Teflon pistons and seals, 0.2 mil Tedlar plastic collapsible bags with Delrin inlet valves, or all-titanium gas-tight samplers with gold seals (Lupton et al., 2008). Free gas bubbles were trapped in a funnel and collected in gas-tight samplers. The sample containers were surrounded by ambient seawater and quickly cooled after collection. Temperature of the fluid flowing into the nozzle and through the manifold during sampling was recorded, allowing calculation of the heat content of the sample. For samples designated with BF or PF in the sample identification number, particles suspended in the flowing water were filtered out and collected on in-line filters. Coarse and heavy particles may have been partially segregated by settling during passage through the manifold. Check valves on container inlets prevented samples from leaking out and pressure relief valves allowed bags and pistons to expand to accommodate excess gas pressure. Standard titanium syringe major samplers (Von Damm 1985) were used on some dives.

Upon arrival on deck, sample containers were removed from the manifold and put into cold storage at 1-5°C. The total gas headspace volume (if present) was measured by removing it into large syringes. An aliquot of gas headspace and fluid was taken for shipboard analysis of H_2 and CH_4 by gas chromatography. Fluid was analyzed on board ship for total dissolved hydrogen sulfide (modified spectrophotometric method of Cline, 1969), pH in closed container with Ross pH electrode, and dissolved silica by spectrophotometry. Sample aliquots were for major ions were filtered through 0.2µm filters and trace metal samples were acidified to pH <2 with ultrapure HCl. Major anions (chloride and sulfate) and cations (Na, K, Mg, Ca) were analyzed by ion chromatography, and in some cases also by titration, ICP-OES, or atomic absorption. Fe, Mn, and Al were analyzed by flame and graphite furnace atomic

absorption on a Perkin Elmer AAnalyst 800. Al was also analyzed by ICP-MS, using matrix-matched standard addition curves and internal standard monitoring on a Perkin Elmer DRC-II or DRC-e. In 2006, sulfite and thiosulfate were analyzed on board ship by preservation/derivitization and liquid chromatography (Vairavamurthy and Mopper, 1990). In 2009, samples were preserved with formaldehyde with minimal air exposure and analyzed on shore for dissolved sulfite (detection limit 20 µmol/kg) and thiosulfate (detection limit 30 µmol/kg) by ion chromatography (Dionex DX500 with AS11HC column, NaOH eluent, and conductivity detection) after removal of >99% of Cl and SO_4 by precipitation in Dionex On-Guard Ag-Ba-H cartridges (method paper in preparation). Thiosulfate was below detection on all formaldehyde-preserved samples analyzed. Sulfate was analyzed in formaldehyde-preserved samples (without removal of Cl/SO_4) to determine the initial sulfate content at the time of preservation. Chromatographic peaks for chloride, sulfite, and sulfate were resolved and samples with millimolar levels of sulfite did not require pre-treatment to remove sulfate. [Sulfate analyzed in non-preserved samples from previous years (Table DR4) gives an approximate measure of the total excess dissolved sulfur species, primarily sulfite and sulfate, after sulfite has oxidized partially or completely to sulfate during sample storage.] Sample J2-401-PF2 collected 4/8/09 with in-situ filtration had a thick pale yellow layer on the filter, assumed to be dominantly elemental sulfur. This material was dried to constant weight (for >two weeks in a dessicator, not under vacuum to avoid sublimation) and weighed on a micro-balance to estimate maximum particulate sulfur content assuming that all material was elemental sulfur. Particulate mass was converted to suspended sulfur concentration using the measured fluid volume passed through the filter. This particular sample had small volume due to sulfur clogging the filter, and no formaldehyde preserved cut was taken. Sulfite was analyzed on 5/22/09 in a sample stored in a tightly capped bottle with no headspace after removal of sulfate and chloride, and total sulfate plus sulfite was analyzed 5/27/09 [results in Table DR1].

The 1-sigma precision of the reported results is: pH, 0.02 pH units; dissolved Si, 2%; Fe and Mn, 4%; Al, 8%; K, Mg, Ca, 1.5%; H_2S, 5%; $SO_4^{=}$, 2%; SO_2(aq), 10%, $S_2O_3^{=}$, 15%.

Titanium gas-tight samples of fluid and free gas were processed at sea and analyzed on shore, and were previously reported (Lupton et al., 2008). The sulfur gas content was calculated by the difference between manometric total gas and total analyzed gas by chromatography. Because only trace H_2S was present in any of the analyzed samples, and no H_2S smell was present in the extracted gas, the sulfur gas is assumed to be SO_2.

To estimate a reasonable primary magmatic gas composition for Figure 2, we took the composition predicted for H_2O, CO_2 and SO_2 from Moretti and Papale (2004) and the high-temperature (750-800°C) H_2 concentration from Saito et al (2002). The primary gas

composition in Figure 2 is an estimate, not a direct measurement of gas at magmatic temperatures.

Submarine arc SO_2 flux calculation. To estimate the magnitude of the SO_2 flux from submarine arc volcanoes, we make a simple calculation as follows. Take the product of the global hydrothermal heat flux for the MOR axis (for crust <1Ma, from Stein and Stein, 1994), the proportion of total hydrothermal heat produced by submarine volcanic arcs from Baker et al., 2008 (10% of MOR flux), the proportion of submarine arc heat produced by eruptions (1/4 to ½ from White et al., 2006), and the average excess sulfur/heat ratio determined from NW Rota volcanic vent fluids. In detail, the numbers are: 3.3×10^{12} J/s x 3600 s/hr x 24 h/d x 365 d/y x 0.1 x 0.25 (or 0.5) x 275 nmol/J x 10^{-9} mol/nmol = 0.7 (to 1.4) x 10^{11} mol of S/y. This is comparable in magnitude to the estimate of 3.15×10^{11} mol SO_2/y for all subaerial arc volcanoes (Fischer, 2008).

References for Supplementary Material

Baker, E.T., Embley, R.W., Walker, S.L., Resing, J.A., Lupton, J.E., Nakamura, K.-I., de Ronde, C.E.J., and Massoth, G.J., 2008, Hydrothermal activity and volcano distribution along the Mariana Arc: Journal of Geophysical Research, v. 113, p. B08S09, doi:10.1029/2007JB005423.

Cline, J., 1969, A spectophotometric method for the determination of dissolved hydrogen sulfide: Limnology and Oceanography, v. 14, p. 454-458.

Deardorff, N. D., K. V. Cashman, and W. W. Chadwick, Jr., 2011, Observations of eruptive plumes and pyroclastic deposits from submarine explosive eruptions at NW Rota-1, Mariana Arc: Journal of Volcanology and Geothermal Research, in press, doi:10.1016/j.jvolgeores.2011.01.003.

Fischer, T.P., 2008, Fluxes of volatiles (H2O, CO2, N2, Cl, F) from arc volcanoes: Geochemical Journal, v. 4p, p. 21-38.

Lupton, J., M. Lilley, D. Butterfield, L. Evans, R. Embley, G. Massoth, B. Christenson, K.-I. Nakamura, and M. Schmidt, 2008, Venting of a separate CO_2-rich gas phase from submarine arc volcanoes: Examples from the Mariana and Tonga-Kermadec arcs: Journal of Geophysical Research, v. 113, B08S12, doi: 10.1029/2007JB005467.

Moretti, R. and P. Papale, 2004, On the oxidation state and volatile behavior in multicomponent gas–melt equilibria: Chemical Geology, v. 213, p. 265-280.

Saito, G., H. Shinohara, and K. Kazahaya, Successive sampling of fumarolic gases at Satsuma-Iwojima and Kuju volcanoes, southwest Japan: Evaluation of short-term variations and precision of the gas-sampling and analytical techniques, *Geochem. J.*, 36, 1-20, (2002).

Stein, C.A. and Stein, S., 1994, Constraints on hydrothermal heat-flux through the oceanic lithosphere from global heat-flow: Journal of Geophysical Research, v. 99, p. 3081-3095.

Vairavamurthy, A. & Mopper, K. Determination of sulfite and thiosulfate in aqueous samples including anoxic seawater by liquid chromatography after derivatization with 2,2'-dithiois(5-nitropyridine). *Environ. Sci. Technol*., 24, 333-337 (1990)

Von Damm, K., Edmond, J.M., Grant, B., Measures, C.I., Walden, B., and Weiss, R.F., 1985, Chemistry of hydrothermal solutions at 21°N, East Pacific Rise: Geochimica et Cosmochimica Acta, v. 49, p. 2197-2220.

White, S.M., Crisp, J.A., and Spera, F.J., 2006, Long-term volumetric eruption rates and magma budgets: Geochemistry Geophysics Geosystems, v. 7, p. Q03010, doi:10.1029/2005GC001002.

Supplementary video caption:

Windows Media Video file (VideoDR1.wmv) extracted from Jason 2 dive 189, April 25, 2006 at 07:04 UT shows an intense bright yellow plume of fine molten sulfur droplets driven up into a rising volcanic plume during a slow lava eruption. This level of activity persisted for more than one hour. We believe this represents slowly ascending lava driving off elemental sulfur accumulated at the top of the lava conduit. Small lava bombs are seen falling back down into the vent. Abundant gas bubbles indicate active magma degassing from the lava conduit. The nearly continuous churning in middle foreground may be caused by seawater boiling in contact with hot rock or by gas bursts through accumulated tephra in the vent. The two red spots are lasers with 10 cm spacing. For details on NW Rota eruption dynamics, see Chadwick et al. 2008 and Deardorff et al., 2011.

TABLE DR1. 2009 FLUID SULFUR CHEMISTRY AT BRIMSTONE VENT

Sample number	Average temperature °C	Heat content relative to ambient J/g	H2S mmol/kg	Sulfite mmol/kg	Initial sulfate mmol/kg	Total excess dissolved sulfur mmol/kg	Excess dissolved sulfur to heat nmol/J
J2 401-P1	37.7	131.1	n.m.	40.1	37.5	49.9	381
J2 401-PF2	49.8	181.4	n.m.	33.3	34.4	39.7	219
J2 401-P3	35.1	120.4	0.002	24.2	35.6	32.1	267
J2 401-P6	201.3	810.1	0.001	133.6	60.5	166.4	205
J2 405-P6	48.0	173.9	0.001	62.0	40.3	74.6	429
J2 405-PF7	46.4	167.2	<0.001	54.6	39.3	66.2	396
J2 403-B24	17.3	46.5	<0.001	2.7	31.7	6.7	144
J2 403-PF4	13.0	28.6	<0.001	2.5	29.7	4.5	156
Brimstone average	50	207	0.001	44	39	55	275
Brimstone std. dev.	59	250	0.001	42	10	52	113
MOR high-T vent average	315.6	1547	7.6	0	0	-20.6	-13

Note: All fluid samples in this table except 401-PF2 were preserved with formaldehyde. Initial sulfate is an upper limit for the sulfate concentration at the time of sampling. Total excess dissolved sulfur is the sum of all dissolved sulfur species minus background seawater sulfate. Negative numbers represent a net loss from seawater. We determined 5.15 mmol/kg particulate sulfur in sample J2-401-PF2 by in-situ filtration followed by drying and weighing. This level of particulate sulfur is 60% in excess of what would be produced by reaction 2 based on the excess sulfate relative to seawater in this sample when it was analyzed. n.m. means not measured.

TABLE DR2. BRIMSTONE VENT SAMPLE INFORMATION

Sample ID	Date collected	Depth m	latitude °N	longitude °E	Sample type
R783-B17	3/30/2004	566	14.5965	144.7777	bag
R783-P20	3/30/2004	549	14.5965	144.7777	piston
R786-B8	4/1/2004	561	14.6008	144.7753	bag
R786-BF11	4/1/2004	561	14.6008	144.7753	filtered bag
R786-P4	4/1/2004	561	14.6008	144.7753	piston
R786-P5	4/1/2004	561	14.6008	144.7753	piston
J2-187-B9	4/23/2006	559.6	14.6009	144.7754	bag
J2-187-PF24	4/23/2006	562	14.6009	144.7754	filtered piston
J2-187MajBlu	4/23/2006	563	14.6010	144.7754	Ti Major
J2-188MajYel	4/24/2006	564	14.6013	144.7764	Ti Major
J2-188MajBlu	4/24/2006	563	14.6009	144.7754	Ti Major
J2-189MajWht	4/25/2006	559	14.5991	144.7778	Ti Major
J2-189MajRed	4/25/2006	560	14.5992	144.7778	Ti Major
J2-191-PF1	4/27/2006	557	14.6010	144.7755	filtered piston
J2-192-BF11	4/28/2006	558.4	14.6009	144.7751	filtered bag
J2-398-PF4	4/5/2009	523.3	14.6008	144.7754	filtered piston
J2-398-P8	4/5/2009	523.3	14.6008	144.7754	piston
J2-398-B24	4/5/2009	523.4	14.6008	144.7754	bag
J2-398-PF2	4/5/2009	524	14.6007	144.7754	filtered piston
J2-401-P1	4/8/2009	523.1	14.6006	144.7753	piston
J2-401-PF2	4/8/2009	523.1	14.6006	144.7753	filtered piston
J2-401-P3	4/8/2009	523.2	14.6006	144.7753	piston
J2-401-P6	4/8/2009	522.8	14.6007	144.7754	piston
J2-403-B24	4/10/2009	519.1	14.6007	144.7753	bag
J2-403-PF4	4/10/2009	519	14.6007	144.7753	filtered piston
J2-403-P1	4/10/2009	519	14.6007	144.7753	piston
J2-405-P3	4/11/2009	521.5	14.6008	144.7754	piston
J2-405-P5	4/11/2009	521.5	14.6008	144.7754	piston
J2-405-PF2	4/11/2009	521.4	14.6008	144.7755	filtered piston
J2-405-B22	4/11/2009	521.5	14.6008	144.7755	bag
J2-405-B21	4/11/2009	521	14.6009	144.7755	bag
J2-405-P6	4/11/2009	521.2	14.6008	144.7755	piston
J2-405-PF7	4/11/2009	521.2	14.6008	144.7754	filtered piston
J2-405-P8	4/11/2009	521.3	14.6008	144.7754	piston
J2-405-PF9	4/11/2009	520.8	14.6008	144.7754	filtered piston
J2-405-BF18	4/11/2009	520.8	14.6008	144.7754	filtered bag

Note: in the sample ID prefix, R=ROPOS and J2=Jason 2. An F in the ID suffix means the sample was filtered through a 0.4 micron filter as it was taken.

TABLE DR3. VOLCANIC VENT FLUID AND BACKGROUND SEAWATER COMPOSITION (1)

Sample ID	Vent	Date collected	Tmax °C	Tavg °C	pH at 22°C	dissolved silica µmol/kg	Fe µmol/kg	Mn µmol/kg
R783b17	Brimstone	3/30/2004	29.8	25.8	2.09	1112	192.5	35.3
R783p20	Brimstone Rim	3/30/2004	16.7	12.8	3.00	388	62.4	11.1
R786p4	Brimstone	4/1/2004	26.1	23.6	2.21	1101	220.4	25.9
R786p5	Brimstone	4/1/2004	29.4	22.6	2.26	838	173.8	20.3
R786b8	Brimstone	4/1/2004	27.1	23.3	2.11	1286	242.8	33.6
R786bf11	Brimstone	4/1/2004	29.5	25.5	1.98	1234	278.2	30.0
J2-187-B9	Brimstone	4/23/2006	28.2	25.4	1.64	n.d.	1616	32.2
J2-187PF24	Brimstone	4/23/2006	95.3	90.2	1.91	550	117	4.66
J2-187MajBlu	Brimstone	4/23/2006	95	n.d.	1.72	3190	2002	35.9
J2-188MajYel	Brimstone	4/24/2006	110	n.d.	1.66	1350	479	9.40
J2-188MajBlu	Brimstone	4/24/2006	95	n.d.	1.05	7060	1873	33.4
J2-189MajWht	Brimstone	4/25/2006	200	n.d.	1.35		808	15.6
J2-189MajRed	Brimstone	4/25/2006	256.6	200	2.11		746	16.7
J2-191-PF1	Brimstone	4/27/2006	41.9	37.6	1.78		473	8.38
J2-407-PF4	Bckgnd SW 581m	4/13/2009	6.4	6.2	7.32	70	<0.09	<0.04
J2-398-PF4	Brimstone	4/5/2009	80.5	53.3	3.80	98	10.9	0.59
J2-398-P8	Brimstone	4/5/2009	31.2	22.5	5.23	94	13.3	0.68
J2-398-PF2	Brimstone	4/5/2009	26.4	22.2	5.86	71	17.9	<0.04
J2-401-P1	Brimstone	4/8/2009	46.9	37.7	1.54	2547	807	16.0
J2-401-PF2	Brimstone	4/8/2009	58.4	49.8	1.62		604	11.6
J2-401-P3	Brimstone	4/8/2009	41.9	35.1	1.66	2581	982	69.9
J2-401-P6	Brimstone	4/8/2009	207.4	201.3	1.06	7032	2737	114
J2-403-B24	Brimstone	4/10/2009	20.5	17.3	3.97	1316	255	21.0
J2-403-PF4	Brimstone	4/10/2009	17.6	13	4.78	577	122	9.33
J2-403-P1	Brimstone	4/10/2009	21.2	18.5	3.65	1431	300	21.7
J2-405-P3	Brimstone	4/11/2009	24.5	20.9	2.27	344	103	2.60
J2-405-P5	Brimstone	4/11/2009	34.7	19	2.25		142	3.48
J2-405-PF2	Brimstone	4/11/2009	44.5	40.6	2.55	273	64.6	1.75
J2-405-B22	Brimstone	4/11/2009	38.7	35.2	1.96	628	188	5.09
J2-405-B21	Brimstone	4/11/2009	21.5	19.2	5.65	257	33.8	7.37
J2-405-P6	Brimstone	4/11/2009	55.7	48	1.49	4280	1108	20.6
J2-405-PF7	Brimstone	4/11/2009	57.9	46.4	1.51	4231	1145	20.9
J2-405-P8	Brimstone	4/11/2009	48.4	41.2	1.43	4037	1043	18.9
J2-405-PF9	Brimstone	4/11/2009	39.5	35.2	1.69	1724	457	10.7
J2-405-BF18	Brimstone	4/11/2009	35.1	28.8	1.96	1295	332	7.19
Brimstone average			59.8		2.4	1819	581	20.5
MOR Hot Vent Average			315.6		3.5	16000	4600	1190.0
Ratio Volc. Vent:MOR			0.19			0.11	0.13	0.02

TABLE DR3. VOLCANIC VENT FLUID AND BACKGROUND SEAWATER COMPOSITION (2)

Sample ID	Fe/Mn	Fe/heat nmol/J	Mn/heat nmol/J	Al µmol/kg	Al/heat nmol/J	K mmol/kg	Mg mmol/kg	Ca mmol/kg
R783b17	5.5	2.5	0.45	67	0.9	10.32	52.64	10.47
R783p20	5.6	2.5	0.45	19	0.8	10.11	55.85	11.16
R786p4	8.5	3.2	0.37	122	1.7	9.81	50.71	9.77
R786p5	8.5	2.7	0.31	96	1.5	9.99	51.57	10.12
R786b8	7.2	3.6	0.49	154	2.3	10.27	52.87	10.16
R786bf11	9.3	3.6	0.39	141	1.8	10.01	51.58	9.89
J2-187B9	50.17	21.05	0.420	1820	23.6	10.18	54.80	12.51
J2-187PF24	25.15	0.34	0.013	115	0.3	8.99	48.76	9.16
J2-187MajBlu	55.80	5.47	0.098	409	1.1	10.38	54.85	9.20
J2-188MajYel	50.92	1.12	0.022	462	1.1	9.70	49.95	10.07
J2-188MajBlu	56.16	5.12	0.091	2558	7.0	8.26	44.26	11.04
J2-189MajWht	51.84	1.01	0.019	661	0.8	9.66	54.13	11.41
J2-189MajRed	44.58	0.70	0.016	376	0.5	9.33	50.12	9.22
J2-191PF1	56.52	3.72	0.066	814	6.4	9.60	52.19	10.31
J2-407-PF4	n.d.	n.d.	n.d.	<0.01	n.d.	9.99	52.39	10.28
J2-398PF4	18.5	0.06	0.00	14.6	0.1	9.79	50.91	9.87
J2-398-P8	19.6	0.20	0.01	9.9	0.2	9.84	52.50	9.85
J2-398-PF2	n.d.	0.27	n.d.	3.1	0.0	9.93	52.01	10.16
J2-401-P1	50.6	6.15	0.12	1412	11.0	9.68	51.59	11.31
J2-401-PF2	52.1	3.33	0.06	1087	6.1	9.79	51.11	10.79
J2-401-P3	14.1	8.16	0.58	1192	10.1	9.75	51.43	10.75
J2-401-P6	24.0	3.38	0.14	2008	2.5	9.15	46.69	11.94
J2-403-B24	12.1	5.49	0.45	1890	43.4	10.25	52.81	10.45
J2-403-PF4	13.1	4.26	0.33	922	35.8	10.08	52.45	10.37
J2-403-P1	13.8	5.83	0.42	2231	45.9	10.21	52.80	10.62
J2-405-P3	39.6	1.68	0.04	106	1.8	9.94	51.95	10.04
J2-405-P5	40.8	2.65	0.07	242	4.8	9.99	52.03	10.14
J2-405-PF2	36.9	0.45	0.01	351	2.5	9.95	52.17	10.08
J2-405-B22	36.9	1.56	0.04	144	1.2	9.93	51.94	10.06
J2-405-B21	4.6	0.62	0.14	64	1.2	10.01	52.65	10.18
J2-405-P6	53.8	6.37	0.12	2156	12.6	9.54	50.13	11.78
J2-405-PF7	54.9	6.85	0.12	1904	11.6	9.59	50.34	11.62
J2-405-P8	55.2	7.16	0.13	1936	13.6	9.52	50.15	11.31
J2-405-PF9	42.7	3.78	0.09	612	5.2	n.d.	n.d.	n.d.
J2-405-BF18	46.2	3.52	0.08	470	5.1	9.92	52.10	10.37
Brimstone Avg.	32.3	3.8	0.19	781.4	5.7	9.8	51.6	10.5
MOR Avg.	4.3	3.10	0.78	5.5	0.0036	22.6	0.0	31.4
Volc:MOR	7.51	1.22	0.24	142	1603	0.43		0.33

TABLE DR4. Sulfur Species in 2004/2006 Volcanic Vent Fluids

	H2S µM	SO4 mM	S2O3 µm	SO2(aq) mM
R786p5	11.7	33.3	n.m.	n.m.
R783p20	25.0	31.0	n.m.	n.m.
R783b17	64.3	34.0	n.m.	n.m.
R786b8	8.8	35.8	n.m.	n.m.
R786p4	5.2	34.4	n.m.	n.m.
R786bf11	3.4	36.9	n.m.	n.m.
R786b17	20.2	27.7	n.m.	n.m.
J2-187B9	bdl	67.7	n.m.	n.m.
J2-187MajBlu	bdl	57.3	79.1	68.9
J2-187PF24	bdl	47.0	0	14.3
J2-188MajBlu	bdl	164.9	n.m.	163.0
J2-188MajYel	bdl	63.7	n.m	21.3
J2-189MajRed	39.6	29.5	n.m.	n.m.
J2-189MajWht	n.m.	44.2	n.m.	49.4
J2-191PF1	bdl	57.1	n.m.	16.7
J2-192BF11	bdl	32.5	n.m.	n.m.

bdl=below detection limit (0.8µM for H_2S). n.m.=not measured.

Supplementary Figures

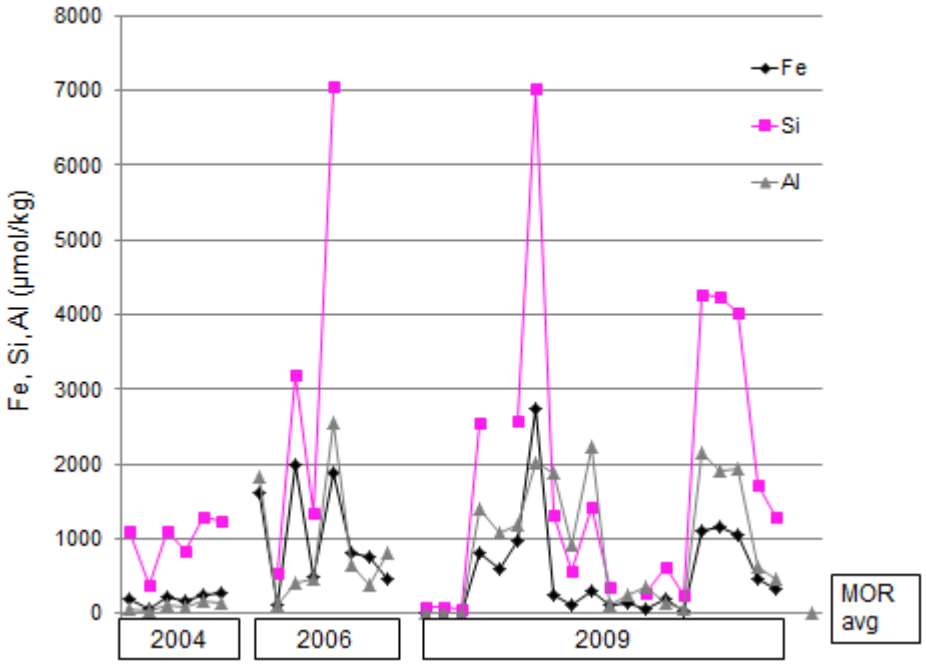

Supplementary Figure DR1. Concentrations of major rock components iron, silica and aluminum dissolved in Brimstone volcanic vent fluids. Samples are in chronological order left to right. Samples show high variability due to variable seawater mixing and extent of reaction with rock substrate. Both the Si/Fe and Al/Fe ratios of these fluids average approximately 50% of the rock ratio, indicative of slower uptake of silica and aluminum into solution and/or solubility limitations. Average Al concentration for high-temperature MOR fluids (5.5µM) is shown at far right for comparison.

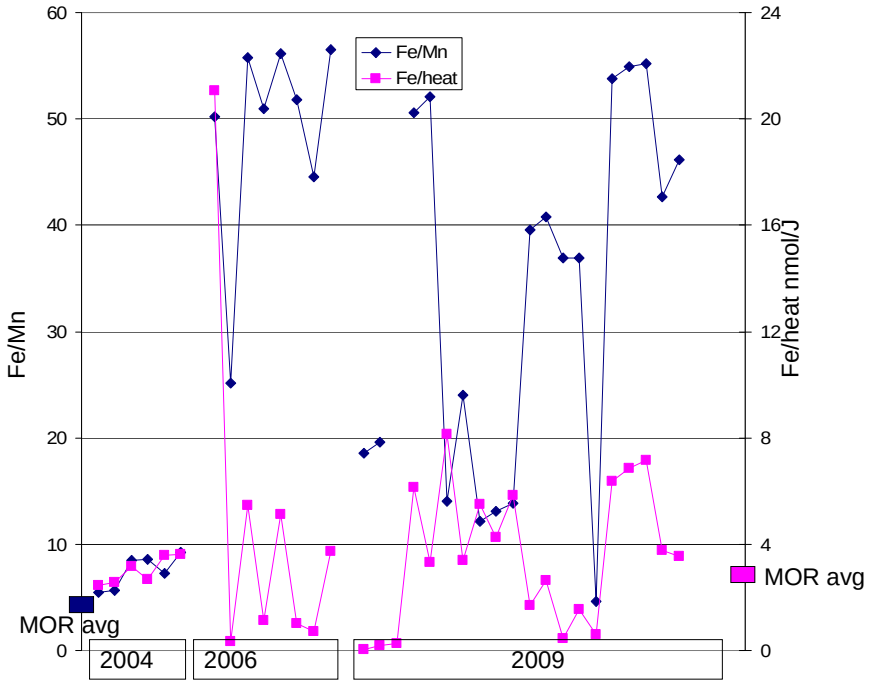

Supplementary Figure DR2. Fe/Mn molar ratio (left axis) and Fe/heat ratio (right axis) in NW Rota volcanic vent fluids. The Fe/Mn ratio (dark blue diamonds) is variable, at times reaching the rock ratio of 55, consistent with congruent dissolution of rock surrounding/covering the eruptive conduit. Lower Fe/Mn ratios indicate solubility limitation and precipitation of secondary iron phases. The average Fe/Mn of all arc volcanic vent samples is 31, considerably higher than the MOR average of 4.3, indicated on the left axis. The Fe/heat ratio is also highly variable, and the overall average of all samples is 3.8, slightly higher than the MOR average of 3.1, shown on the right axis. The near equality of Fe/heat ratios in arc volcanic vents and MOR vents means that they have the same relative importance for global iron flux to the oceans. The flux of Mn from volcanic vents is considerably less than that from MOR vents.

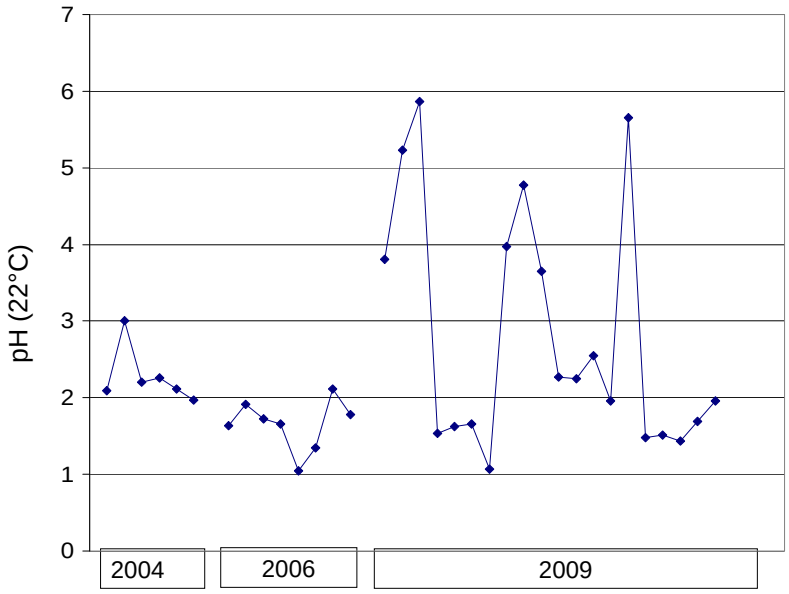

Supplementary Figure DR3. pH (measured shipboard at 22°C) in volcanic vent fluids from Brimstone eruptive vent. Data are in chronological order left to right. 2004 samples are more dilute because they were taken in a buoyant plume within the eruptive pit crater.

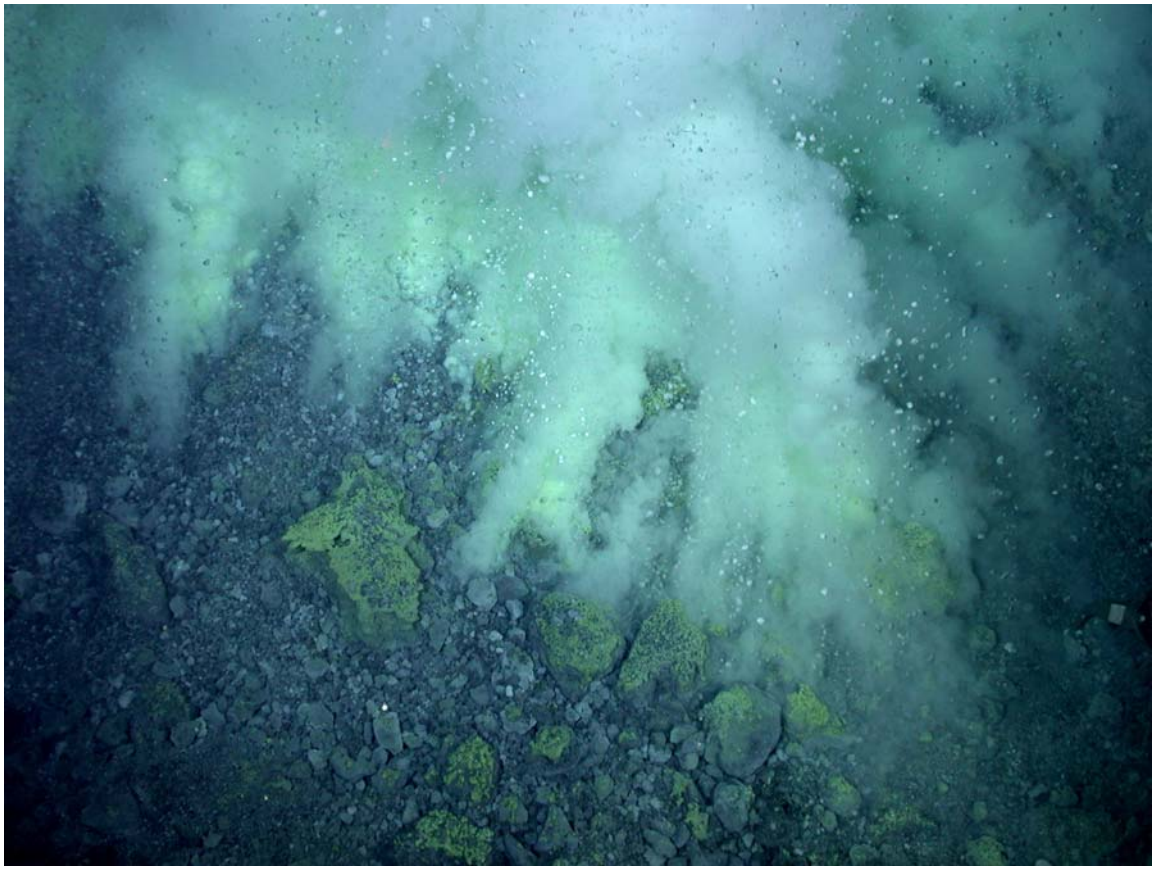

Supplementary Figure DR4. NW Rota, Brimstone vent, 2006, Jason-2 dive 188. Gas bubbles, white and yellow sulfur-rich particles venting through volcaniclastic material, including rocks coated with sulfur. Note that yellow smoke is proximal to the volcanic vent, with white smoke and gas bubbles on the distal edges. Temperature probe measurements beneath the white smoke were less than the melting point of sulfur (~115°C). Molten sulfur is present beneath yellow smoke, with temperatures from 120 to 256°C measured.

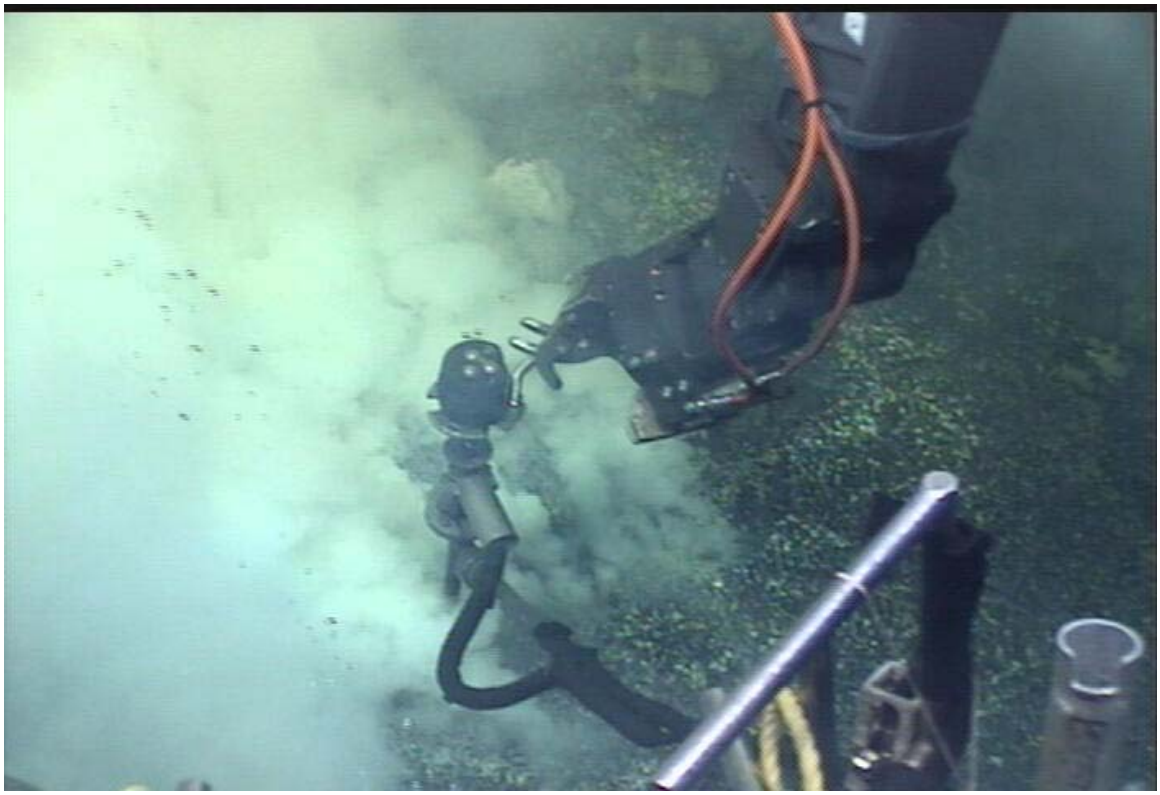

Supplementary Figure DR5. Sampling fluids with HFPS nozzle in sulfur-rich volcaniclastic material on the edge of Brimstone eruptive vent, dive J2-401, 4/8/2009. In-line fluid temperatures were 25-60°C at this spot beneath white smoke. Minutes later, in a spot beneath yellow smoke approximately 30cm away from this location, fluid temperatures up to 207°C, with pH of 1.05 were measured.

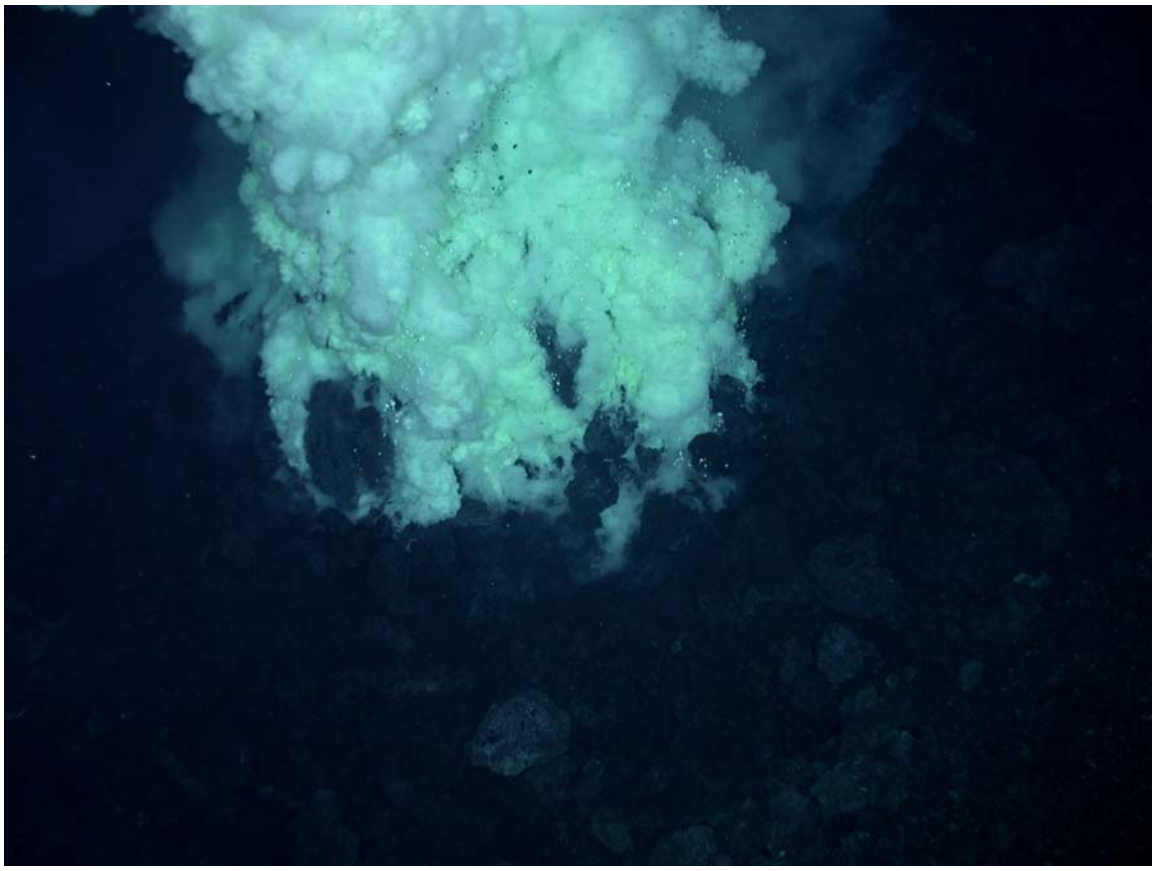

Supplementary Figure DR6. NW Rota 2006, Brimstone vent. Slowly extruding lava plug giving off yellow and white sulfur smoke and gas bubbles, indicative of active magma degassing during extrusion. Temperature measured on the surface of one of these “smoking rocks” reached 256°C, near the seawater boiling point of 265° at 550m depth.

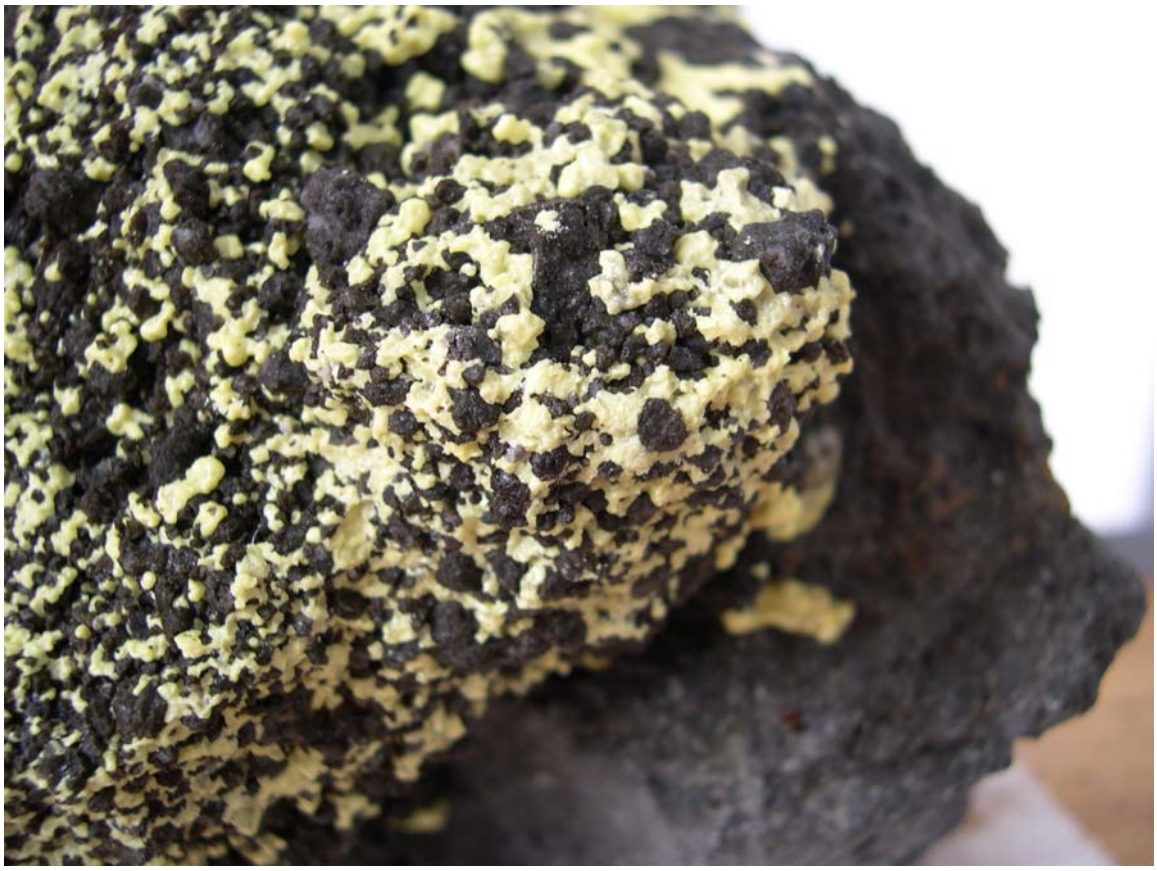

Supplementary Figure DR7. Rock collected near Brimstone vent, NW Rota, 2006. Sample is a lava bomb with one side coated with cemented breccia of sulfur and volcaniclastic basaltic andesite. This is indicative of lava ascending and erupting through a sulfur cap, pushing molten sulfur up through loose material covering the vent. (Field of view is 7x11cm).